In Vivo MR Evaluation of Age-Related Increases in Brain Iron

George Bartzokis, Jim Mintz, David Sultzer, Peter Marx, James S. Herzberg, C. Kelly Phelan, and Stephen R. Marder

PURPOSE: To assess the validity of an MR method of evaluating tissue iron. **METHODS:** The difference between the transverse relaxation rate (R_2) measured with a high-field MR instrument and the R_2 measured with a lower field instrument defines a measure termed the *field-dependent R_2 increase* (FDRI). Previous in vivo and in vitro studies indicated that FDRI is a specific measure of tissue iron stores (ferritin). T2 relaxation times were obtained using two clinical MR instruments operating at 0.5 T and 1.5 T. T2 relaxation times were measured in the frontal white matter, caudate nucleus, putamen, and globus pallidus of 20 healthy adult male volunteers with an age range of 20 to 81 years. R_2 was calculated as the reciprocal of T2 relaxation time. These in vivo MR results were correlated with previously published postmortem data on age-related increases of nonheme iron levels. **RESULTS:** The FDRI was very highly correlated with published brain iron levels for the four regions examined. In the age range examined, robust and highly significant age-related increases in FDRI were observed in the caudate and putamen. The correlations of age and FDRI in the globus pallidus and white matter were significantly lower and did not have statistical significance. **CONCLUSIONS:** The data provide additional evidence that FDRI is a specific measure of tissue iron stores. The data also show that age-related increases in tissue iron stores can be quantified in vivo despite significant age-related processes that oppose the increase in R_2 caused by iron. These results are relevant to the investigation of neurodegenerative processes in which iron may catalyze toxic free-radical reactions.

Iron; Brain, magnetic resonance; Brain, growth and development; Magnetic resonance, tissue characterization; Age and aging

AJNR Am J Neuroradiol 15:1129–1138, Jun 1994

The extrapyramidal system contains the highest concentration of iron in the brain. Levels range from one-and-a-half to almost twice as high as that in the liver (1). Up to 90% of nonheme iron in the brain is in the iron-stage protein ferritin (1–3). The ferritin complex consists of a multisubunit protein shell (apoferritin) surrounding a crystalline core of hydrous ferric oxide that may be made up of as many as 4500 ferric iron atoms (4).

An association between high iron levels and central nervous system damage has been observed in a variety of disorders, and iron involvement in the process of lipid peroxidation has been suggested as a common mechanism (5–8). An in vivo method that quantifies physiologic forms of iron with specificity may therefore have clinical and research value in evaluating neurodegenerative disorders (9–13).

Brain extrapyramidal nuclei exhibit shorter T2 relaxation time than other gray matter. T2 shortening seems to be related to the high iron concentrations in the extrapyramidal nuclei (9–12, 14–17). Drayer (18) pointed out that multiple lines of evidence support an association between T2 shortening and tissue iron levels. First, many investigators have observed T2 shortening in disorders with known abnormal iron accumulation of brain and liver (9, 11, 12, 19–22). Second,

Received May 21, 1993; accepted pending revision August 23; revision received September 7.

Presented in part at the 12th Annual Meeting of the Society of Magnetic Resonance in Medicine, New York, August 1993. Supported in part by the Research Service of the Department of Veterans Affairs, National Alliance for Research on Schizophrenia and Depression, the Scottish Rite Schizophrenia Research Program, and National Institute of Mental Health Grant 5T32-MH-17140.

From the Research Service (G.B., J.S.H.) and the Psychiatry Service (G.B., J.M., D.S., S.R.M.), West Los Angeles VA Medical Center; Department of Psychiatry, University of California Los Angeles (G.B., J.M., D.S., C.K.P., S.R.M.); and Department of Radiology, Harbor-University of California Los Angeles, Torrance (G.B.).

Address reprint requests to George Bartzokis, MD, West Los Angeles VA Medical Center, Brentwood Division, 11301 Wilshire Blvd, Mail Code B-151H, Los Angeles, CA 90073.

AJNR 15:1129–1138, Jun 1994 0195-6108/94/1506-1129

some postmortem studies have reported that T2 shortening corresponded to increased iron levels (9–12, 14). Third, age-related increases in brain iron demonstrated in postmortem studies of healthy humans (1, 23–25) are similar to age-related T2 shortening observed in vivo (26–30). However, the ability of MR to quantify iron levels in vivo remains controversial (18): some investigators report a lack of correlation between postmortem tissue iron levels and T2 values (31–33), and there are contradictory reports on whether age-related changes in brain T2 parameters plateau in adulthood or continue into old age (27–30).

Ferritin has been shown to exert a strong magnetic effect that results in marked T2 shortening in vivo and in vitro (17, 22, 34–37). Field dependence of tissue T2 parameters has also been observed in vivo and in vitro (15, 17, 37–41). Ferritin, which is ubiquitous in tissues (4), has been shown to shorten T2 more in high-field instruments than in low-field instruments (17, 40), and this field-dependent effect seems specific to ferritin (17). Recently, Bartzokis et al (17) reported a method that exploits the field-dependent effects of ferritin on T2 to quantify ferritin in vivo with specificity. The method consists of measuring T2 on two different field-strength instruments, calculating the transverse relaxation rate R_2 ($R_2 = 1/T2 \times 1000$), and evaluating the difference in R_2 (high-low field), termed *field-dependent R_2 increase* (FDRI).

There are multiple possible explanations for the FDRI caused by ferritin. One explanation is that the field inhomogeneity created by the heterogeneous distribution of paramagnetic ferric iron atoms in the ferritin core increases the observed R_2 to a greater extent in higher than in lower field strength instruments. This is the same explanation given for the field-dependent R_2 increases observed in stationary red blood cells (42, 43). Other explanations involve special properties that may be unique to iron in a crystalline form. The small microcrystalline ferric oxide structures in the ferritin complex (4) may exhibit a variety of magnetic behaviors such as ferromagnetism, antiferromagnetism (44, 45), and superparamagnetism (46). Regardless of the mechanism producing the observed FDRI, iron in the form found in ferritin, and in quantities found in normal human brain, contributes markedly and specifically to the FDRI measured with clinical magnetic resonance (MR) instruments (17).

Here we present the application of the FDRI method to the evaluation of age-related iron deposit increases in a group of healthy volunteers and assess the validity of the FDRI method by correlating in vivo MR results with previously published postmortem data on age-related increases in nonheme levels of iron (1).

Methods

Subjects

Twenty-three healthy adult male volunteers recruited from the community and hospital staff participated in the study after giving informed consent. Subjects were excluded if there was a family history of Alzheimer disease, Huntington disease, or other neurodegenerative disorders, or a history of head trauma that resulted in loss of consciousness for longer than 15 minutes. These criteria excluded three subjects from the analysis (two with abnormal motor exam and one with a family history of Alzheimer disease). One patient with a family history of Parkinson disease was included because of the low genetic risk for this disease.

The remaining 20 subjects ranged in age from 20 to 81 years (mean, 55.5, SD, 18). All but one subject were right-handed. All scored in the normal range on the Mini-Mental State Examination (47) and on the Unified Parkinson's Disease Rating Scale (48).

MR Protocol

All subjects were scanned using the same two instruments (1.5-T and 0.5-T Picker instruments, Cleveland, Ohio), and both scans were done the same day using the same imaging protocol.

Two pilot sequences were obtained to specify the location and spatial orientation of the head and the position of the axial image acquisition grid. First, a coronal pilot spin-echo image 100/30/1 (repetition time/echo time/excitations), 10-mm thickness, was acquired and used to align the subsequent sagittal pilot images. The first section of the image-acquisition grid of the sagittal pilot images was aligned on the coronal pilot in order to image a true midsagittal section of brain. Second, the sagittal pilot spin-echo images 550/26/2, 5-mm thickness, were acquired.

Finally, the midsagittal image was used to position the axial image acquisition grid, as described in the next section. The axial image acquisition sequence acquired interleaved contiguous sections using a Carr Purcell Meiboom Gill dual spin-echo sequence 2500/20,90/2, 192 gradient steps, 3-mm section thickness, and 25-cm field of view.

Head and Image Section Positioning

The coronal and sagittal pilot scans obtained before the axial image acquisition were used to determine the accuracy of repositioning the head in the second MR instrument

and to make adjustments in head position if necessary. The adjustments continued until the head was repositioned to within 5 mm of the position used to acquire the first MR study. The accuracy of head repositioning was ensured by measuring the displacement of the apex of the third ventricle (visualized in the coronal pilot) and the anterior commissure (visualized in the midsagittal pilot) in the high-field scan from the low-field scan.

After a symmetrical (as determined by laser light crosshairs) and comfortable head position was achieved, tape was applied to the forehead of the subject in order to reduce the likelihood of head displacement between the three sequences (coronal, sagittal, and axial). In addition, a comfortable semirigid pillow that formed a mold of the back and sides of the subject's own head was used. These steps minimized shifts in the position of the head during the image acquisition and helped ensure that the location and spatial orientation of the head was the same in the two scanners, because the same molded pillow was used in both scanners.

To position the actual image sections identically within the brain and thus sample the same volume of tissue, we used the sagittal pilot scan. The axial section select grid was adjusted so that the anterior commissure was contained within the same section in both high- and low-field instruments. This procedure ensured that the midsection of the anterior commissure was clearly visible in one of the subsequent axial sections. For increased consistency all subsequent measures were referenced to this section (48).

Image Analysis

T2-weighted images were calculated using Picker system software. T2 was calculated for each voxel by an automated algorithm from the two signal intensities (echo time = 20 and 90) of the dual spin-echo sequence to produce gray-scale–encoded T2 maps of the brain as demonstrated in Figure 1.

The T2 measures were extracted using an Apple (Cupertino, Calif) Macintosh configured image analysis work station that reads optical disks containing the original MR data stored in digital format. Morphometric (area) and T2 measures were then obtained in a semiautomated way using software for the Apple Macintosh work station (Company for Quantitative Imaging, Los Angeles, Calif).

A single rater trained in the use of the image analysis software and the recognition of the regions of interest obtained all the measurements. The rater had no knowledge of the purpose of the study, the way the data were subsequently used, or any clinical information on the subjects.

The image analysis software permits the rater to delineate the structures of interest using a mouse. The contour of the head of the caudate, putamen, globus pallidus, and frontal white matter was drawn manually by the rater using the gray/white matter contrast of the early echo (echo time = 20) images. When necessary, the data contained in the sections before and after the section being measured and the late echo (echo time = 90) images were used to help define the borders of the structures of interest. Thus, on images on which a border was ambiguous, the rater could follow the border from a section of unambiguous delineation to the more difficult section being rated. The region of interest is then "pasted" onto the T2 image and, with the histogram and "shrink image" functions, any areas with a T2 greater than 130 msec were removed before recording the final gray matter area (Figs 1A and 1B).

Partial voluming of cerebrospinal fluid in a voxel containing mostly brain tissue can markedly increase the T2 of the voxel. Therefore, in an effort to obtain a T2 measure of homogeneous "cerebrospinal fluid–free" brain tissue, we eliminated all pixels with values that fell above the right side (higher T2 values) inflection point on the histogram distribution of the region of interest (Fig 1B). The inflection point was defined as the point on the right half of the distribution contour that separates the curve concave downward from the curve concave upward. Thus, most pixels containing even small partial volumes of cerebrospinal fluid were removed; the final measure was the average T2 for the remaining homogeneous region of brain tissue (Fig 1C).

T2 data for each of the four regions of interest were obtained from contiguous pairs of sections. The section containing the anterior commissure and the section immediately superior to it were used to obtain the putamen and globus pallidus T2 data (Fig 1). The third and fourth sections above the anterior commissure were used to obtain the T2 data for caudate nucleus and frontal lobe white matter. The average T2 of the two sections and the 6-mm-thick volume of the two sections were the raw data. R_2 was calculated as the reciprocal of T2 × 1000. The average R_2 and the sum of the volumes of the two hemispheres were the final measures used in the subsequent analyses.

Results

Correlations Between FDRI and Brain Iron Concentrations

The R_2 data from the individual subjects are displayed in Figure 2. Data from the 20 subjects were analyzed using a 4 × 2 within-subject repeated measures analysis of variance. Within-subject factors were brain region (frontal white matter, caudate, putamen, and globus pallidus) and field strength (0.5 T and 1.5 T). The region-x field-strength interaction was significant (multivariate analysis of variance, $F = 104.14$, df = 3.17, $P = .0001$, repeated measures analysis of variance, $F = 199.03$, df = 3.57, $P = .0001$).

Subsequently, follow-up statistical tests within and between regions were performed. As shown in Table 1, the increase in R_2 at the higher field strength was significant in all four brain regions, using the *t* test for correlated samples.

Pairwise contrasts were computed, comparing the FDRI across the four brain regions. Even the

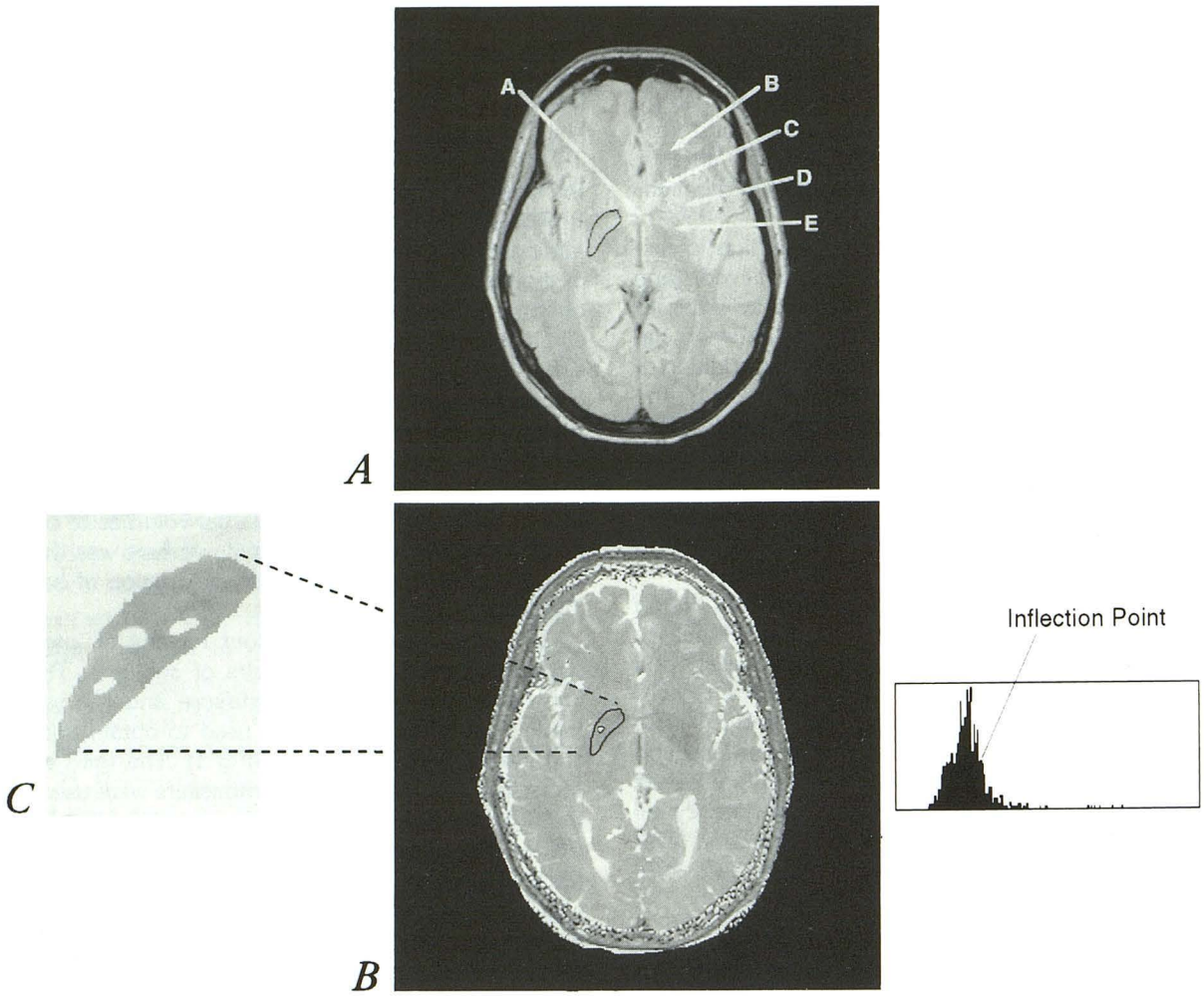

Fig. 1. *A*, For a basal ganglia region of interest like the globus pallidus, the operator manually delineates the structure using the contrast on the early echo (echo time 20) of the dual spin-echo sequence 2500/20,90/2. *A* indicates anterior commissure; *B*, frontal white matter; *C*, caudate; *D*, putamen; and *E*, globus pallidus.

B, Because the region of interest may contain cerebrospinal fluid intensity pixels, the region of interest is pasted on the T2 image; pixels with a T2 value greater than 130 msec are eliminated before the area measurement is recorded. To obtain the T2 measurement, all region of interest pixels with values above the inflection point of the histogram distribution are eliminated.

C, The resulting T2 value is representative of the remaining homogeneous tissue of the region of interest, free of partial volume effects caused by small areas of hyperintensity.

smallest difference (caudate versus putamen FDRI) was significant ($t = 2.65$, $P = .016$). For all the remaining comparisons, the FDRI for each structure was highly significantly different from all other structures ($t > 7.23$, $P > .0001$).

The correlation between the average FDRI for the 20 subjects and published brain nonheme iron concentrations observed in frontal white matter, caudate, putamen, and globus pallidus (4.24, 9.28, 13.32, and 21.3 mg iron/100 g tissue, respectively) of normal adult human brain (1) was $r = .962$, df = 2, $P = .0385$.

Correlation Between FDRI and Age

We examined the relationship between age and FDRI in a correlation analysis. The results (Table 2) show highly significant correlations between age and FDRI in two of the four regions of interest (caudate and putamen). The scatterplots of these data in the caudate and putamen (Fig 3) indicated that these correlations were not unduly influenced by outliers.

The correlations between the R_2 values obtained in the four regions of interest and age at each of two field strengths (0.5 T and 1.5 T) are displayed in Table 3. These correlations suggest that FDRI may be a more specific measure of iron stores than high-field R_2 alone. This is because the high-field magnet may be sensitive to two different aging processes, one of which is associated with *increasing* R_2, and the other with *decreasing* R_2. In caudate and putamen, high-field

Figure 2. BRAIN $R_2 (\frac{1}{T_2})$ VALUES

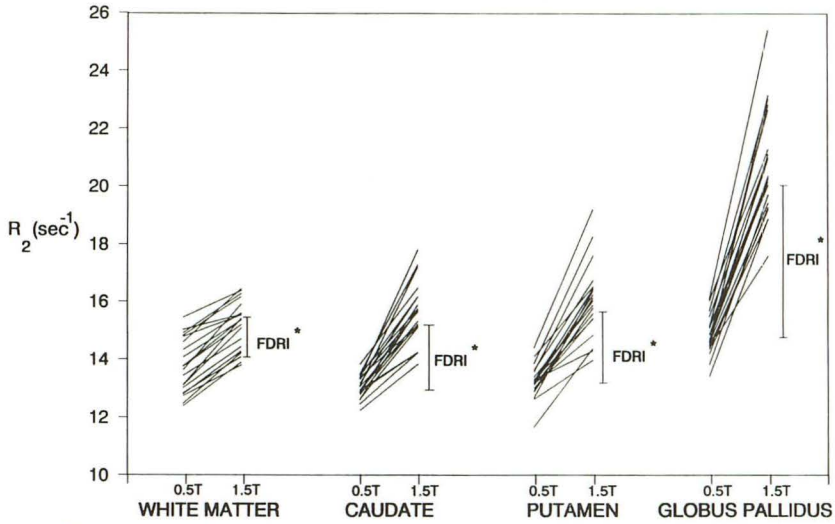

* Field Dependant R_2 Increase (FDRI) defined as the difference in the means of calculated R_2 values obtained using the two field strength instruments(0.5T AND 1.5T).

TABLE 1: Brain R_2 values at two field strengths

Region	Field Strength, T	R_2 Values,[a] Mean (SD)	FDRI Difference[b]
White matter	1.5	15.48 (.676)	1.38 (t = 12.1, p = .0001)
	0.5	14.10 (.741)	
Caudate	1.5	15.18 (.698)	2.24 (t = 20.0, p = .0001)
	0.5	12.94 (.401)	
Putamen	1.5	15.71 (.833)	2.47 (t = 15.4, p = .0001)
	0.5	13.23 (.326)	
Globus Pallidus	1.5	20.04 (1.31)	5.29 (t = 21.3, p = .0001)
	0.5	14.76 (.646)	

[a] Means from 20 subjects (age 20 to 81 years) examined with both 0.5-T and 1.5-T instruments. R_2 in seconds^{-1}.

[b] Field-dependent R_2 increase (FDRI) difference is defined as the difference between the means of calculated R_2 values for each brain region obtained using the two field-strength instruments.

TABLE 2: Correlations of age with FDRI across brain[a]

	Caudate	Putamen	Globus Pallidus	White Matter
r	.76	.77	.34	.29
P	.0001	.0001	.14	.21

[a] Field-dependent R_2 increase (FDRI) is defined as the difference between the R_2 values for each brain region obtained using the two field-strength MR instruments.

R_2 increased strongly with age, as would be expected if it were measuring increasing iron content. However, high-field R_2 decreased significantly in white matter, suggesting that it also is affected by a second aging process that presumably is unrelated to iron storage, such as myelin loss or water increase (30, 33, 41).

As seen in Table 3, low-field R_2 seems to be a relatively pure measure of this second process. In white matter, it decreases with age even more strongly than the high-field measure. However, it shows virtually none of the tendency to increase with age in caudate or putamen. Thus, it provides a basis for correction of the high-field reading, subtracting variance associated with non–field-dependent changes.

The specificity of the FDRI method is graphically shown in Figure 4, which displays the regression lines of age versus the R_2 at both field strengths and the FDRI for the four regions of interest.

We used multiple regression analyses to evaluate the correlation between R_2 and age when data from the high- and low-field-strength magnets were combined, and to estimate the optimal weights to maximize that correlation. For the regression coefficients in caudate and putamen regions, these weights are roughly equal, opposite in sign (low-field negatively correlated and high-field positively correlated with age), and statistically significant, suggesting that a simple difference score (ie, the FDRI) is close to the optimal weighting. In the caudate and putamen, the high-field R_2 was significantly and positively associated with age ($P < .0002$). In all four regions the multivariate analysis indicated that low-field R_2 was significantly and inversely associated with age ($P < .05$). This suggests that, in all four regions, the low-field magnet provides a more specific measure of age-related processes that are unrelated to iron stores and decrease R_2 with age. In the age range examined, adding information from the high-field-strength magnet did not im-

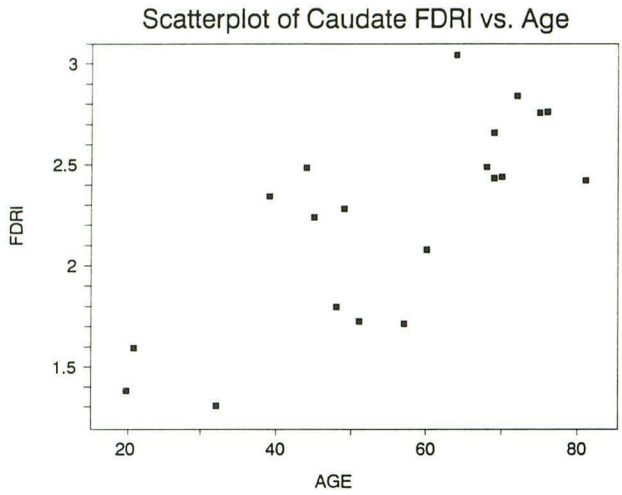

3A

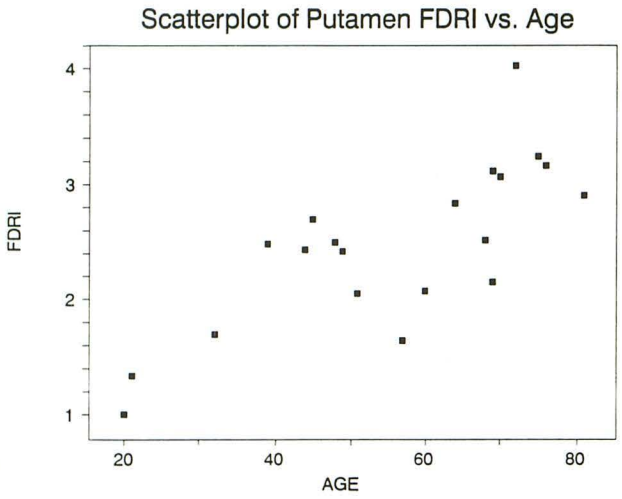

3B

TABLE 3: Correlations of age with R_2, determined using high- and low-field-strength MR instruments across brain regions

Field Strength		Caudate	Putamen	Globus Pallidus	White Matter
0.5 T	*r*	.17	.08	−.32	−.65
	P	.48	.74	.17	.0017
1.5 T	*r*	.64	.69	.13	−.50
	P	.0023	.0007	.57	.0262

prove the correlation in the globus pallidus and the white matter regions.

In the age range examined, the correlations of age with FDRI in caudate and putamen were significantly higher ($P < .05$) than in white matter and globus pallidus (Table 2 and Fig 4). In fact, the modest correlations in the latter two regions seemed to be entirely attributable to the two subjects' being in their 20s. When these two were deleted and the correlations recomputed using only subjects older than 30, results were still highly significant in the caudate ($r = .66$, $P < .01$, df = 16) and putamen ($r = .61$, $P < .01$, df = 16), but the correlations fell essentially to zero in globus pallidus ($r = .12$, not significant) and white matter ($r = -.06$, not significant). Similar results were obtained even when the analyses were based only on those subjects older than 40. Thus, as documented in Figure 3, age-related increases in iron continue well past middle age in the caudate and putamen. This observation is consistent with postmortem data, suggesting that maximum values of iron for caudate and putamen are reached after the 40s, as compared with the 30s in the rest of the extrapyramidal system and white matter (1).

On analysis of the morphometric data, a significant correlation between age and the volume of the putamen was observed ($r = -.5269$, $P = .0170$). The caudate and globus pallidus volumes were not significantly correlated with age ($r = -.0225$, $r = -.2370$, respectively). When the correlations of age versus FDRI were reevaluated with the effect of volume partialed out, the putamen correlation was lowered but remained robust and statistically significant ($r = .6539$, $P = .0010$). The caudate and globus pallidus correlations remained essentially unchanged.

Measurement Reliability

Test-retest reliability of the FDRI measurements was assessed by computing intraclass correlation coefficients on two ratings of six scans done 1 month apart by the same rater. The statistic was computed by estimating variance components associated with between-subject and within-subject variability. The coefficients reflect the proportion of total variance accounted for by differences among subjects (SAS Proc VARCOMP). Significance of the intraclass correlations was determined using the general linear model, with subjects forming the grouping factor (SAS Proc GLM). Reliability was very good for the caudate ($r_{xx} = .981$, $F = 105$, $P < .0001$), putamen ($r_{xx} = .946$, $F = 36.1$, $P < .0002$), globus pallidus ($r_{xx} = .995$, $F = 377$, $P < .0001$), and white matter ($r_{xx} = .877$, $F = 15.26$, $P < .0023$).

Discussion

The data demonstrate robust and highly significant age-related increases in FDRI in the caudate and putamen. These age-related increases in iron stores are specific to the caudate and putamen

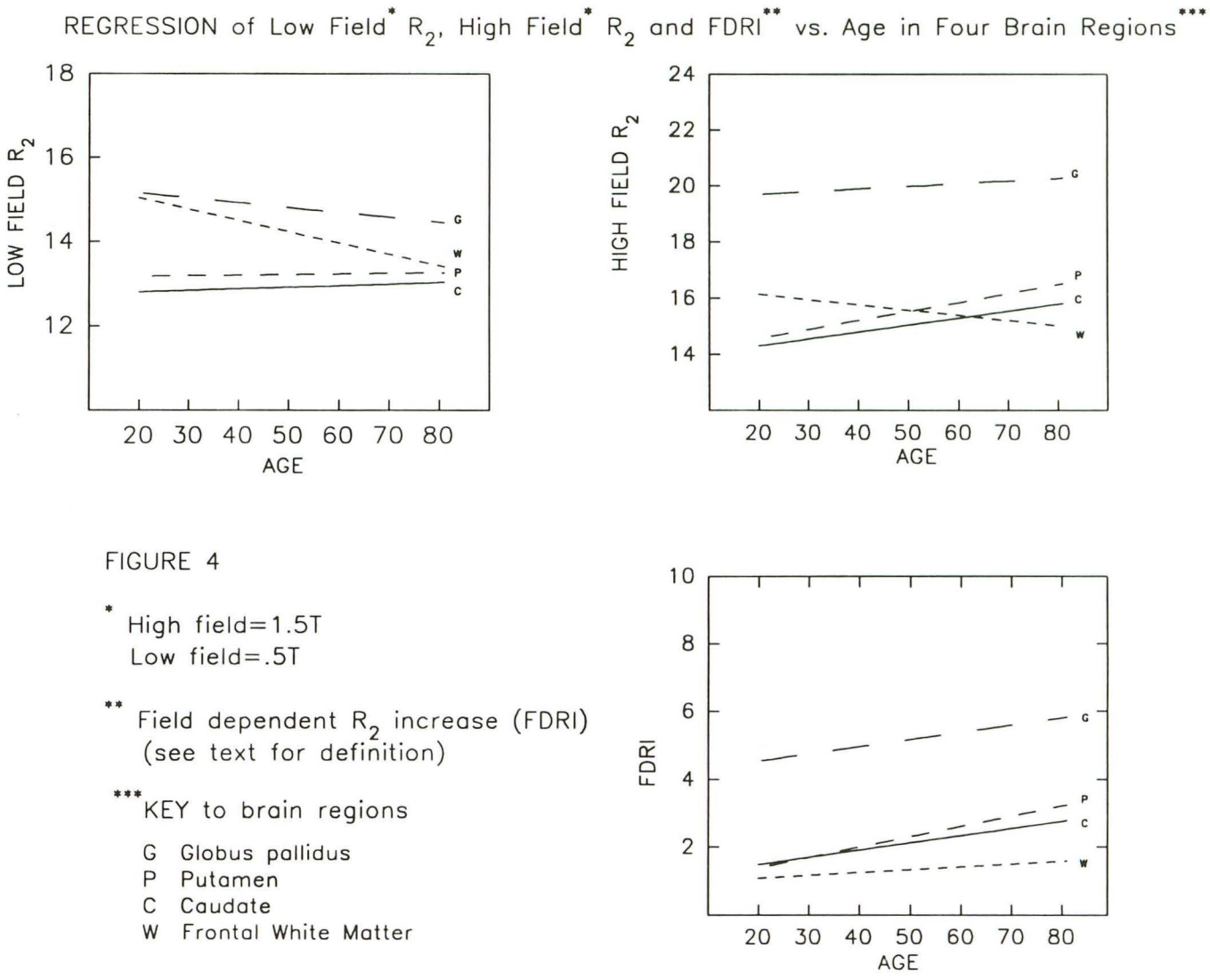

FIGURE 4

* High field=1.5T
Low field=.5T

** Field dependent R_2 increase (FDRI) (see text for definition)

*** KEY to brain regions

G Globus pallidus
P Putamen
C Caudate
W Frontal White Matter

of adults because, in this age range, globus pallidus and white matter FDRI increased significantly less with age despite significant age-related changes in white matter R_2 measures.

The data confirm that the R_2 values obtained with high-field clinical instruments are more sensitive to the iron content of tissue than low-field-strength instruments (14) and that FDRI can be observed and quantified with clinical MR instruments operating at field strengths of 0.5 T and 1.5 T (17). The FDRI of the four brain structures examined is very highly correlated with published nonheme iron concentrations of adult brain (1). Thus, the data strengthen the evidence that R_2 values obtained with high-field clinical instruments are affected by the ferritin content of tissue, and that FDRI may be useful as a specific quantitative measure of tissue ferritin content (17).

In addition, the data show that although age-related changes in R_2 relaxation times can be detected with high-field MR instruments alone, a stronger and more specific relationship is observed with the FDRI method (Tables 2 and 3). The specificity of the FDRI for ferritin is highlighted by comparing white matter FDRI with basal ganglia FDRI. White matter has high-field-independent R_2 processes (probably related to the myelin content) as indicated by the high R_2 values obtained for this tissue with both 0.5- and 1.5-T instruments relative to the basal ganglia R_2 values (Figs 2 and 4). The FDRI method eliminates these field-independent R_2 effects and shows white matter to have the lowest FDRI of the four regions, which is consistent with postmortem data on nonheme iron levels (1, 25). In addition, there is a robust and statistically significant age-related decrease in R_2 observed in white matter with both

the high- and low-field-strength instruments (Table 3). This is probably related to a diffuse age-related loss of myelin and/or increased water content and not to age-related "loss" of iron. The FDRI method eliminates these field-independent age-related R_2 decreases and reveals only a negligible age-related rise in white matter FDRI (Table 2), which is again consistent with postmortem data on nonheme iron levels (1, 25).

The age-related decrease in white matter R_2 has been previously reported (50), and it demonstrates the presence of other field-independent age-related processes that oppose the age-related R_2 increase caused by increasing iron deposits. This observation is of technical importance because it suggests that MR methods of evaluating iron deposits that use white matter intensity values as a reference or correction factor (15, 28) may be affected by these complex and concomitant age-related processes.

The specificity of the FDRI method is also suggested by a close examination of the globus pallidus data (Tables 2 and 3 and Fig 4). The negative correlation of globus pallidus R_2 with age on the low-field instrument again suggests that globus pallidus water content may increase with age, thus causing an age-related decrease in R_2. On the other hand, the high-field-strength instrument does not seem to show this process. These observations could be explained by a small concomitant age-related increase in iron levels, suggested by the modest age-related increase in FDRI (Table 2) and nonheme iron levels (1), in this age range. Thus, in the high-field instrument, the age-related increase in R_2 caused by increasing iron levels would oppose the age-related decrease in R_2 (demonstrated by the low-field instrument), resulting in the apparent absence of any age-related trends.

Multiple tissue changes such as increased water content can be expected in normal aging (30) and other neurodegenerative disorders as tissue is destroyed (51, 52). The specificity provided by the FDRI method may prove useful in investigating the role of iron in neurodegenerative disorders because single-field-strength instrument measurements of R_2 have often been disappointing (30, 33, 41).

Several limitations need to be acknowledged before further comments. Our sample size is small, and the presence of some curvilinearity to the age-related FDRI increases cannot be ruled out. The data were obtained from a small (6-mm-thick) sample of the region of interest; different relationships may be detected if the structures are evaluated in their entirety or if other portions of the structures are evaluated. We were unable to assess the detailed nature of age-related increases in FDRI in a variety of field strengths because only two field-strength instruments were available. In addition, in a cross-sectional study of normal aging only limited inferences can be made about the significance of the results to pathologic conditions. Nevertheless, the data show that clinical instruments can provide T2 measurements, which even if not accurate in absolute terms, can be reliably measured and can provide useful quantification of FDRI.

Some postmortem and MR studies conclude that the age-related increases in the iron levels of most brain regions reach a plateau in adulthood (1, 29, 30); others suggest that the increases in iron stores in the basal ganglia continue into the 80s (25, 27, 28). In evaluating cross-sectional data on healthy aging one must keep in mind that an apparent plateau in iron levels in the older age group may actually be a "ceiling effect." This effect may be substantial if brain iron levels are themselves associated with mortality and/or neurologic conditions that cause subjects to be excluded from participating in a study of normal aging. In the current study this effect may have attenuated some or all of the age-FDRI and age-R_2 relationships.

We attempted to evaluate whether the increased iron is simply a marker for age-related cell loss that results in higher iron concentrations (27, 53), or whether the iron contributes to the pathogenesis of disease processes and normal aging, as others have suggested (8, 13, 54–57). We were able to detect an age-related reduction in size of the putamen (50, 58). When the correlations of age with FDRI were reevaluated with the effect of volume partialed out, the putamen correlation was lowered but remained robust and statistically significant. The caudate and globus pallidus correlations remained essentially unchanged. Thus, the age-related increase in FDRI could not be solely explained by reduction in the volume's causing an increase in the iron concentration of the structure. More definitive answers to the question of whether increased rates of brain atrophy are related to increased iron levels must await prospective studies.

There are many possible clinical applications for an in vivo method of specifically quantifying iron stores at the millimeter resolution provided by MR. The central nervous system is at espe-

cially high risk for damage from free radical neurotoxic metabolic processes catalyzed by iron (59, 60). Thus, increased iron levels may have significant pathophysiologic consequences, which are manifested as different clinical phenomena depending on which brain region is most affected. The involvement of iron and free radical neurotoxic processes has in fact been postulated for a variety of age-related neuropsychiatric disorders such as Parkinson disease (33, 55, 56), Alzheimer disease (8, 53, 54, 57, 61), Huntington disease (25, 33), tardive dyskinesia (13), and possibly the process of brain aging itself (57). Because the increase in brain iron is age-related (1, 23–30), the role of iron in all age-related neurodegenerative disorders deserves investigation. If a causal relationship is demonstrated, new avenues of treatment and prevention of these diseases would be possible (62). In addition, serial evaluations of FDRI could be used to monitor iron chelating treatments (63) which are currently used in patients with transfusion hemosiderosis and have been tentatively shown to be effective in the treatment of some patients with Alzheimer disease (62).

Using MR imaging, in vivo evaluation of the role of iron in neurodegenerative disorders is now possible because field-independent changes in R_2 can be eliminated through the FDRI method. Because ferritin is present in all tissues, the above discussion could be generalized to other organs, especially those with relatively high iron concentrations, such as the liver, spleen, and muscle. Additional work is necessary to define further the specificity of iron in the form found in ferritin as the sole or major contributor to FDRI and to delineate the quantitative relationship between ferritin levels and FDRI.

Acknowledgments

We thank William H. Oldendorf, MD, Joseph Tabrisky, MD, and Michael Goldstein, PhD, for their support, Diane Osborne and W. Thomas Ellis for technical assistance, and Sun Sook Hwang and Heraclio Avila for assistance in preparing the manuscript.

References

1. Hallgren B, Sourander P. The effect of age on the non-haem iron in the human brain. *J Neurochem* 1958;3:41–51
2. Hill JA. The distribution of iron in the brain. In: Youdum MBH, ed. *Brain iron: neurochemical and behavioral aspects.* London: Taylor & Francis 1988:1–24
3. Morris CM, Candy JM, Leith AB, et al. Brain iron homeostasis. *J Inorganic Biochem* New York: Wiley, 1992;47:257–265
4. Theil EC. The ferritin family of iron storage proteins. In: Nord FF, Meister A, eds. *Advances in enzymology and related areas of molecular biology.* New York: Wiley, 1990;63:421–429
5. Park BE, Netsky MG, Betsill WL. Pathogenesis of pigment and sphenoid formation in Hallevorden-Spatz syndrome and related disorders: peroxidation as a common mechanism. *Neurology* 1975;25:1172–1178
6. Sadeh M, Sandbank U. Neuraxonal dystrophy and hemosiderin in the central nervous system. *Ann Neurol* 1980;7:286–287
7. Kim RC, Ramachandran T, Parisi JE, Colins GH. Pallidonigral pigmentation and sphenoid formation with multiple striatal lacunar infarcts. *Neurology* 1981;31:774–777
8. Connor JR, Menzies SL, St. Martin SM, Mufson EJ. A histochemical study of iron, transferin, and ferritin in Alzheimer's disease brains. *J Neurosci Res* 1992;31:75–83
9. Duguid JR, De La Paz R, DeGroot J. Magnetic resonance imaging of the midbrain in Parkinson's disease. *Ann Neurol* 1986;20:744–747
10. Drayer BP. Magnetic resonance imaging and brain iron: implications in the diagnosis and pathochemistry of movement disorders and dementia. *BNI Quat* 1987;3:15–30
11. Coffey EC, Alston S, Heinz ER, Burger PC. Brain iron in progressive supranuclear palsy: clinical, magnetic resonance imaging, and neuropathological findings. *J Neuropsych Clin Neurosci* 1989;1:400–404
12. Schaffert DA, Johnsen SD, Johnson PC, Drayer BP. Magnetic resonance imaging in pathologically proven Hallervorden-Spatz disease. *Neurology* 1989;39:440–442
13. Bartzokis G, Garber HJ, Marder SR, Oldendorf WH. MRI in tardive dyskinesia: shortened left caudate T2. *Biol Psychiatry* 1990;28:1027–1036
14. Drayer BP, Burger P, Darwin R, Riederer S, Herfkens R, Johnson GA. MRI of brain iron. *AJNR Am J Neuroradiol* 1986;147:103–110
15. Bizzi A, Brooks RA, Brunetti A, et al. Role of iron and ferritin in MR imaging of the brain: a study in primates at different field strengths. *Radiology* 1990;177:59–65
16. Higgins JJ, Patterson MC, Papadopoulos NM, Brady RO, Pentchev PG, Barton NW. Hypoprebetalipoproteinemia, accanthocytosis, retinitis pigmentosa, and pallidal degeneration (HARP syndrome). *Neurology* 1992;42:194–198
17. Bartzokis G, Aravagiri M, Oldendorf WH, Mintz J, Marder SR. Field dependent transverse relaxation rate increase may be a specific measure of tissue iron stores. *Magn Reson Med* 1993;29:459–464
18. Drayer BR. Basal ganglia: significance of signal hypointensity on T2-weighted images. *Radiology* 1989;173:311–312
19. Brasch RC, Wesbey GE, Gooding CA, Koerper MA. Magnetic resonance imaging of transfusional hemosiderosis complicating thalasimia major. *Radiology* 1984;150:767–771
20. Gomori JM, Grossman RI, Bilaniuk LT, Zimmerman RA, Goldberg HI. High-field MR imaging of superficial siderosis of the central nervous system. *J Comput Assist Tomogr* 1985;9:972–975
21. Johnston DL, Rice L, WesleyVick G, Hedrick TD, Rokey R. Assessment of tissue iron overload by nuclear magnetic resonance imaging. *Am J Med* 1989;87:40–47
22. Thulborn KR, Sorensen GA, Kowall NW, et al. The role of ferritin and hemosiderin in the MR appearance of cerebral hemorrhage: a histopathologic biochemical study in rats. *AJNR Am J Neuroradiol* 1990;154:291–297
23. Gans A. Iron in the brain. *Brain* 1923;46:128–136
24. Diezel PB. Iron in the brain: a chemical and hystochemical examination. In: Waalsch H, ed. *Biochemistry of the developing nervous system.* New York: Academic Press, 1955:145–152
25. Klintworth GK. Huntington's chorea—morphologic contributions of a century. *Adv Neurol* 1973;1:353–368
26. Aoki S, Okada Y, Nishimura K, et al. Normal deposition of brain iron in childhood and adolescence: MR imaging at 1.5 T. *Radiology* 1989;172:381–385

27. Olanow CW, Holgate RC, Murtaugh R, Martinez C. MR imaging in Parkinson's disease and aging. In: Crane DB, ed. *Parkinsonism and aging*. New York: Raven Press, 1989:155–164
28. Milton WJ, Atlas SW, Lexa FJ, Mozley PD. Deep gray matter hypointensity patterns with aging in healthy adults: MR imaging at 1.5 T. *Radiology* 1991;181:715–719
29. Pujol J, Junque C, Vendreli P, et al. Biological significance of iron-related magnetic resonance imaging changes in the brain. *Arch Neurol* 1992;49:711–717
30. Schenker C, Meier D, Wichmann W, Boiesiger P, Valavanis A. Age distribution and iron dependency of the T2 relaxation time in the globus pallidus and putamen. *Neuroradiology* 1993;35:119–124
31. Chen JC, Hardy PA, Clauberg M, et al. T2 values in the human brain: comparison with quantitative assays of iron and ferritin. *Radiology* 1989;173:521–526
32. Brooks DJ, Luthert P, Gadian D, Mardsen CD. Does signal-attenuation on high-field T2-weighted MRI of the brain reflect regional cerebral iron deposition? Observations on the relationship between regional cerebral water proton T2 values and iron levels. *J Neurol Neurosurg Psychiatry* 1989;52:108–111
33. Chen JC, Hardy PA, Kucharczyk W, et al. MR of human postmortem brain tissue: correlative study between T2 and assays of iron and ferritin in Parkinson and Huntington disease. *AJNR Am J Neuroradiol* 1993;14:275–281
34. Koenig SH, Baglin CM, Brown RD. Magnetic field dependance of solvent proton relaxation in aqueous solutions of Fe^{3+} complexes. *Magn Reson Med* 1985;2:283–288
35. Koenig SH, Brown RD, Gibson JF, Ward RJ, Peters TJ. Relaxometry of ferritin solutions and the influence of the Fe^{3+} core ions. *Magn Reson Med* 1986;3:755–767
36. Gillis P, Konig SH. Transverse relaxation of solvent protons induced by magnetized spheres: application to ferritin, erythrocites, and magnetite. *Magn Reson Med* 1987;5:323–345
37. Brittenham GM, Farrell DE, Harris JW, et al. Magnetic-susceptibility measurements of human iron stores. *N Engl J Med* 1982;307:1671–1675
38. Dockery SE, Suddarth SA, Johnson GA. Relaxation measurements at 300 Hz using MR microscopy. *Magn Reson Med* 1989;11:182–192
39. Bernardino ME, Chaloupka JC, Malko JA, Chezmar JL, Nelson RC. Are hepatic and muscle T2 values different at 0.5 and 1.5 Tesla? *Magn Reson Imaging* 1989;7:363–367
40. Vymazal J, Brooks RA, Zak O, McRill C, Shen C, Di Chiro G. T1 and T2 of ferritin at different field strengths: effect on MRI. *Magn Reson Med* 1992;27:368–374
41. Malisch TW, Hedlund LW, Suddarth SA, Johnson GA. MR microscopy at 7.0 T: effects of brain iron. *J Magn Reson Imaging* 1991;1:301–305
42. Brooks RA, Di Chiro G. Magnetic resonance imaging of stationary blood: a review. *Med Phys* 1987;14:903–913
43. Gomori JM, Grossman RI, Yu-Ip C, Asakura T. NMR relaxation times of blood: dependance on field strength, oxidation state, and cell integrity. *J Comput Assist Tomogr* 1987;11:684–690
44. Blaise A, Chappert J, Girardet JL. Observation par mesures magnetique et effet Mossbauer d'un antiferromagnetisme de grains fins dans la ferritine. *C R Hebdomadaires Seanc Acad Sci* 1965;261D:2310–2313
45. Boas JF, Window B. Mossbauer effect in ferritin. *Aust J Phys* 1966;19:573–576
46. Neel L. Superparamagnetisme des grain tres fins antiferomagnetiques. *C R Hebdomadaires Seanc Acad Sci* 1961;252B:4075–4080
47. Folstein MF, Folstein SE, McHugh PR. "Mini-Mental State": a practical method for grading the cognitive state of patients for the clinician. *J Psychiatry Res* 1975;12:189–198
48. Motgomery GK. PD and the Columbia scale. *Neurology* 1984;34:557–558
49. Naidich TP, Daniels DL, Perch P, Haughton VM, Williams A, Pojunas K. Anterior commissure: anatomic-MR correlation and use as a landmark in three orthogonal planes. *Radiology* 1986;158:421–429
50. Jernigan TL, Archibald SL, Berhow MT, Sowell ER, Foster DS, Hesselink JR. Cerebral structure on MRI, I: localization of age-related changes. *Biol Psychiatry* 1991;29:55–67
51. Bondareff W, Raval J, Colletti PM, Hauser DL. Quantitative magnetic resonance imaging and the severity of dementia in Alzheimer's disease. *Am J Psychiatry* 1988;145:853–856
52. Besson JAO, Crawford JR, Parker DM, et al. Multimodal imaging in Alzheimer's disease. The relationship between MRI, SPECT, cognitive and pathological changes. *Br J Psychiatry* 1990;157:216–220
53. Hallgren B, Sourander P. The non-haem iron in the cerebral cortex in Alzheimer's disease. *J Neurochem* 1960;5:307–310
54. Goodman L. Alzheimer's disease: a clinico-pathologic analysis of twentythree cases with a theory on pathogenesis. *J Nerv Ment Dis* 1953;117:97–130
55. Youdim MBH, Ben-Shachar D, Yehuda S, Riederer P. The role of iron in the basal ganglion. *Adv Neurol* 1990;53:155–162
56. Jellinger K, Paulus W, Grundke-Iqbal I, Riederer P, Youdim MBH. Brain iron and ferritin in Parkinson's and Alzheimer's diseases. *J Neural Trans* 1990;2:327–340
57. Stadtman ER. Metal ion-catalyzed oxidation of proteins: biochemical mechanisms and biological consequences. *Free Radic Biol Med* 1990;9:315–325
58. Schwartz M, Creasey H, Grady CL, et al. Computed tomographic analysis of brain morphometrics in 30 healthy men, aged 21 to 81 years. *Ann Neurol* 1985;17:146–157
59. Halliwell B, Gutteridge JMC. The importance of free radicals and catalytic metal ions in human diseases. *Mol Aspects Med* 1985;8:89–193
60. Halliwell B, Gutteridge JMC. Iron as biological pro-oxidant. *ISI Atlas Sci Biochem* 1988;1:48–52
61. Bartzokis G, Sultzer D, Mintz J, et al. MRI suggests increased brain iron in Alzheimer's disease. *Biol Psychiatry* 1994 (in press).
62. McLachlan DRC, Dalton AJ, Kruck TPA, et al. Intramuscular desferrioxamine in patients with Alzheimer's disease. *Lancet* 1991;337:1304–1308
63. Andersen PB, Birgegard G, Nyman R, Hemmingsson A. Magnetic resonance imaging in idiopathic hemochromatosis. *Eur J Haematol* 1991;47:174–178